Atmospheric and Oceanic Science Letters xxx (xxxx) xxx

KeAi CHINESE ROOTS GLOBAL IMPACT

Contents lists available at ScienceDirect

Atmospheric and Oceanic Science Letters

journal homepage: http://www.keaipublishing.com/en/journals/atmospheric-and-oceanic-science-letters/

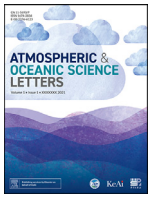

Strong heatwaves with widespread urban-related hotspots over Africa in 2019

Eghosa Igun[a,b], Xiyan Xu[a], Yonghong Hu[c], Gensuo Jia[a,b,*]

[a] Key Laboratory of Regional Climate-Environment for East Asia, Institute of Atmospheric Physics, Chinese Academy of Sciences, Beijing, China
[b] University of Chinese Academy of Sciences, Beijing, China
[c] Key Laboratory of Digital Earth Science, Aerospace Information research Institute, Chinese Academy of Sciences, Beijing, China

ARTICLE INFO

Keywords:
Africa
Temperature
Heat wave
Urban hotspots
Population
关键词:
非洲
温度
热浪
城市热点
人口

ABSTRACT

2019 was one of the hottest years in recent decades, with widespread heatwaves over many parts of the world, including Africa. However, as a developing and vulnerable region, the understanding of recent heatwave events in Africa is limited. Here, the authors incorporated different climate datasets, satellite observations, and population estimates to investigate patterns and hotspots of major heatwave events over Africa in 2019. Overall, 2019 was one of the years that experienced the strongest heatwaves in terms of intensity and duration since 1981 in Africa. Heatwave hotspots were clearly identified across western-coastal, northeastern, southern, and equatorial Africa, where major cities and human populations are located. The proportion of urban agglomerations (population) exposed to extreme (99th percentile) heatwaves in the Northern Hemisphere and Southern Hemisphere rose from 4% (5 million people) and 15% (17 million people), respectively, in the baseline period of 1981–2010 to 36% (43 million people) and 57% (53 million people), respectively, in 2019. Heatwave patterns and hotspots in 2019 were related to anomalous seasonal change in atmospheric circulation and above-normal sea surface temperature. Without adaptation to minimize susceptibility to the effects of heatwave events, the risks they pose in populated areas may increase rapidly in Africa.

摘要

2019 年是近几十年来最热的年份之一, 包括非洲在内的全球许多地区都受到大范围的热浪侵袭. 然而, 非洲作为脆弱的发展中地区, 我们对其近年热浪事件的了解非常有限. 本研究中, 我们结合了不同的气候数据集, 卫星观测资料和人口数据, 研究了 2019 年非洲地区主要热浪事件发生的时空特征和热点分布区. 总体而言, 2019 年是非洲地区自 1981 年以来热浪强度最强, 持续时间最久的年份之一. 在主要城市和人口所在的非洲西海岸, 东北部, 南部和赤道地区是热浪发生的热点区. 位于赤道以北的非洲地区, 暴露于极端 (第 99 个百分位) 热浪的城市人口比例从 1981–2010 年基准期的 4% (500 万人) 上升至2019 年的 36% (4300 万人). 位于赤道以南地区, 暴露于极端热浪的城市人口则从基准期的15% (1700 万人) 上升至57% (5300 万人). 2019 年的热浪时空特征和热点分布与大气环流的季节变化异常和海温的暖异常有关. 如果不及时采取适应措施以尽量减少人口对热浪事件影响的敏感性, 热浪对非洲人口稠密地区构成的风险可能会迅速增加.

1. Introduction

Heatwave events are marked by periods of extremely high above-normal temperatures that have far-reaching societal, economic, and environmental impacts on global, regional, and local scales (Russo et al., 2014). Because of increasing exposure to higher temperatures due to heatwave events, heat stress is becoming more severe globally, with greater impacts on ecosystems and human society (Brooke and Bell, 2011). In order to design appropriate adaptive measures, it is critical to assess spatial patterns of recent heat events and identify hotspot areas (Wilhelmi and Hayden, 2010).

Africa has been identified as one of the continents with increasing exposure to heatwave events due to climate change (Nangombe et al., 2019). Over the second half of the 20th century, a rise in heatwaves and a decrease in cold spells were reported in the Sahel and West African regions (Moron et al., 2016). In the past few decades, significant increases in the frequency and duration of heatwave events have been noted over Africa (Engelbrecht et al., 2015). Climate projections for the 21st century also expect further increases in hot extremes over some parts of Africa (Driouech et al., 2020). Generally, the focus of most of these studies has been on certain parts of Africa, or future projections of heatwave events. It is, however, valuable to examine recent heatwave events over the entire continent, particularly their spatial link with ur-

* Corresponding author.
E-mail address: jiong@tea.ac.cn (G. Jia).

https://doi.org/10.1016/j.aosl.2022.100195
Received 14 January 2022; Revised 8 February 2022; Accepted 18 February 2022
Available online xxx

Please cite this article as: E. Igun, X. Xu, Y. Hu et al., Strong heatwaves with widespread urban-related hotspots over Africa in 2019, Atmospheric and Oceanic Science Letters, https://doi.org/10.1016/j.aosl.2022.100195

ban areas at higher risk due to the significant economic activities carried out there and the populations residing in them.

According to the temperature records from the World Meteorological Organization (WMO), 2019 was among one of the warmest years globally since 1850. However, the magnitude of these recent heatwave events in 2019 has not been investigated in Africa, and particularly in its urban areas, which are currently undergoing a rapid rise in population and with poor adaptive capacity (Rohat et al., 2019). Here, we focused on understanding the spatial patterns, hotspots, and associated mechanisms of recent heatwave events in 2019. Overall, the objectives of this study were to (1) quantify how strong the 2019 heatwave events were compared to the 1981–2010 baseline period, (2) identify hotspots of heatwave events and their connections with urban agglomeration, and (3) assess possible associated mechanisms.

2. Data and methods

2.1. Data

Datasets of near-surface daily maximum temperature, monthly 850-hPa geopotential height (HGT), monthly 850-hPa wind, monthly volumetric soil water (0–10 m) (soil moisture), and monthly total precipitation from the ERA5 reanalysis were used to assess heatwave events. We obtained these datasets from 1981 to 2019 at a spatial resolution of 0.25° × 0.25°. The ERA reanalysis dataset, archived by the European Centre for Medium-Range Weather Forecasts, provides hydrometeorological variables at different spatial and temporal scales and has been progressively used to tackle a number of issues relating to climate risk assessment to date (Weedon et al., 2014).

We acquired collection-6 daily land surface temperature (LST) products (MYD11A1) at a spatial resolution of 1 km, derived from the Moderate Resolution Imaging Spectroradiometer (MODIS) onboard the Aqua satellite. We used this dataset to assess the background conditions. This dataset comprises clear-sky observations of daytime temperatures from 2002 to 2019, with an overpass time of 1330 local time (representing the daily maximum temperature). This LST product has been improved to avoid biases through the correction of noise as a result of cloud cover, changes in zenith angle, and topography differences, and its data quality reaches a root-mean-square error of ±1 K in most cases (Wan, 2008).

We also obtained global sea surface temperature (SST) data (1981–2019) from HadISST4 at a spatial resolution of 1° × 1° (Huang et al., 2015). In addition, urban agglomeration and population datasets were acquired from the United Nations Department of Economic and Social Affairs population division (https://population.un.org/wpp/Download/Standard/Population/; accessed in January 2021). This study adopted the definition of urbanized areas from the United Nations (population ≥ 0.05 million persons) to identify urban areas.

2.2. Evaluation of heatwave events

We identified a heatwave as having occurred when there were three or more consecutive days with a daily maximum temperature above a percentile-based threshold. The threshold used in this study was the 95th percentile of daily maxima, based on a 15-day moving window. Using a moving window accounts for temporal dependence while producing a reasonable sample size to calculate a realistic percentile value (Perkins and Alexander, 2013).

We assessed two heatwave metrics: (i) heatwave intensity (HWI) and (ii) heatwave duration (HWD). The HWI is the exceedance of maximum daily temperature for each heatwave event, while the HWD is the cumulative days of each heatwave event. These heatwave metrics were estimated for four seasons, including austral summer (December–January–February, DJF), boreal summer (June–July–August, JJA), austral fall (March–April–May, MAM), and austral spring (September–October–November, SON). Annual heatwave events were estimated from the combination of all four seasons. In accounting for changes in the spatial distribution of temperature and heatwave events in 2019, anomalies were computed relative to the baseline period (1981–2010). The chosen baseline period follows the WMO definition (Arguez and Vose, 2011). To enhance our understanding of the contrasting heatwave patterns, we considered the seasonality of the northern and southern parts, and hence the continents were divided into two main areas: the Northern Hemisphere (NH) (0°–38°N, 18°W–55°E) and Southern Hemisphere (SH) (0°–35°S, 10°–55°E) (Fig. 1(a)).

2.3. Identification of hotspots associated with urban clusters

The comparison between maximum temperature anomalies of ERA5 and MODIS LST revealed good consistency between both datasets from 2002 to 2019, with a correlation coefficient of 0.83 and 0.89 in the NH and SH, respectively (Fig. 1(b, c)). Hence, MODIS LST was also used to evaluate heatwave hotspots because it shows better information about the heterogeneity of background conditions. We identified heatwave hotspots as regions where the tail of the temperature distribution warmed faster (above the 95th, 97th, and 99th percentiles) than the rest of the temperature distribution (Lewis et al., 2019). We categorized hotspot areas as strong (95th percentile), severe (97th percentile), and extreme (99th percentile) (Hobday et al., 2018). These are critical levels of impacts and risk assessment for human health and ecosystems. We overlaid urban agglomerations on hotspot areas in order to estimate the fraction of urban agglomeration areas affected by heatwave events in 2019.

2.4. Associated heatwave wave mechanisms

Possible mechanisms associated with heatwave events in 2019 were examined by computing seasonal anomalies relative to the baseline period (1981–2010) for 850-hPa HGT, 850-hPa wind, soil moisture, precipitation, and SST. We first estimated global SST anomalies before correlating the SSTs in the proximity of Africa (42°N–40°S, 25°W–65°E) with the heatwave events in 2019. To avoid bias in the results, datasets were detrended before computing anomalies. Generally, positive and negative values of HGT anomalies indicate an increase and decrease in surface warming, respectively (Jézéquel et al., 2018). The pattern correlation between the anomalies of HGT and HWI in 2019 was also computed.

3. Results

3.1. Patterns and magnitudes of heatwaves in 2019

We examined the change in maximum temperature (Fig. S1(a–c)) and heatwave events (Fig. 1(d–g)) in 2019 relative to the baseline period (1981–2010). Maximum temperatures of over 1°C were observed across 99% of land areas, with major intensification in the SH (up to 8°C) (Fig. S1(a, c)). The NH and SH experienced extended HWI (HWD) by 1.7°C (33 days) and 3.3°C (67 days), respectively (Fig. 1(d–g)). Overall, 2019 was one of the years with the strongest heatwaves in terms of intensity and duration over Africa since 1981 (Fig. S2(a–d)).

In relation to the baseline period, the heatwave magnitude increased across all seasons in 2019 over Africa with varying spatial distribution. However, the strongest heatwave events were observed in austral summer (DJF), with 60% of the total land area in Africa affected (Fig. 2(a)). Relative to the baseline period, the heatwave events in DJF increased in HWI (HWD) by 1.8°C (8 days) and 3°C (24 days) in the NH and SH, respectively. Heatwave events in boreal summer (JJA) impacted 42% of the total land area over Africa and had an HWI (HWD) of 1.7°C (29 days) and 0.8°C (8 days) in the NH and SH, respectively (Fig. 2(b, f)). Heatwaves observed in austral fall and austral spring impacted 57% (Fig. 2(c)) and 41% (Fig. 2(d)) of the total land area, respectively.

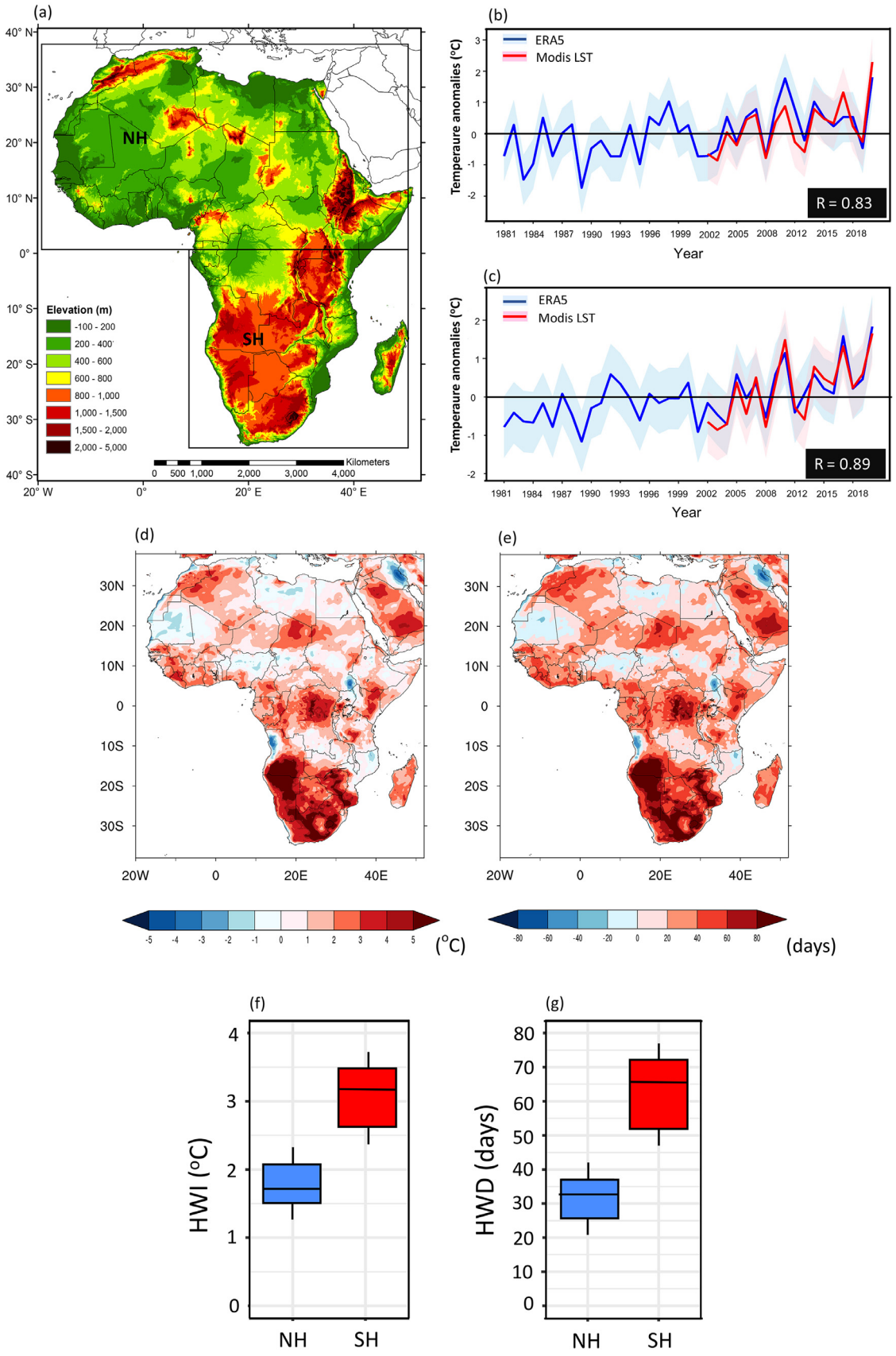

Fig. 1. Subdivision of Africa, annual mean of maximum daily temperature, and heatwave events in 2019. (a) 0° to 38°N is the NH, while 0° to 35°S is the SH. Time series of annual mean maximum daily temperature anomalies of MODIS LST (red) (2002–2019) and ERA5 (blue) (1981–2019) in the NH (b) and SH (c). The pink and blue shading denotes confidence intervals for the lower 5th and upper 95th percentiles. (d) The 2019 anomalous HWI relative to the 1981–2010 baseline. (e) The 2019 anomalous HWD relative to the 1981–2010 baseline. Box-and-whisker plots indicate the 10th, 25th, 50th, 75th, and 90th quantiles of (f) HWI and (g) HWD in 2019.

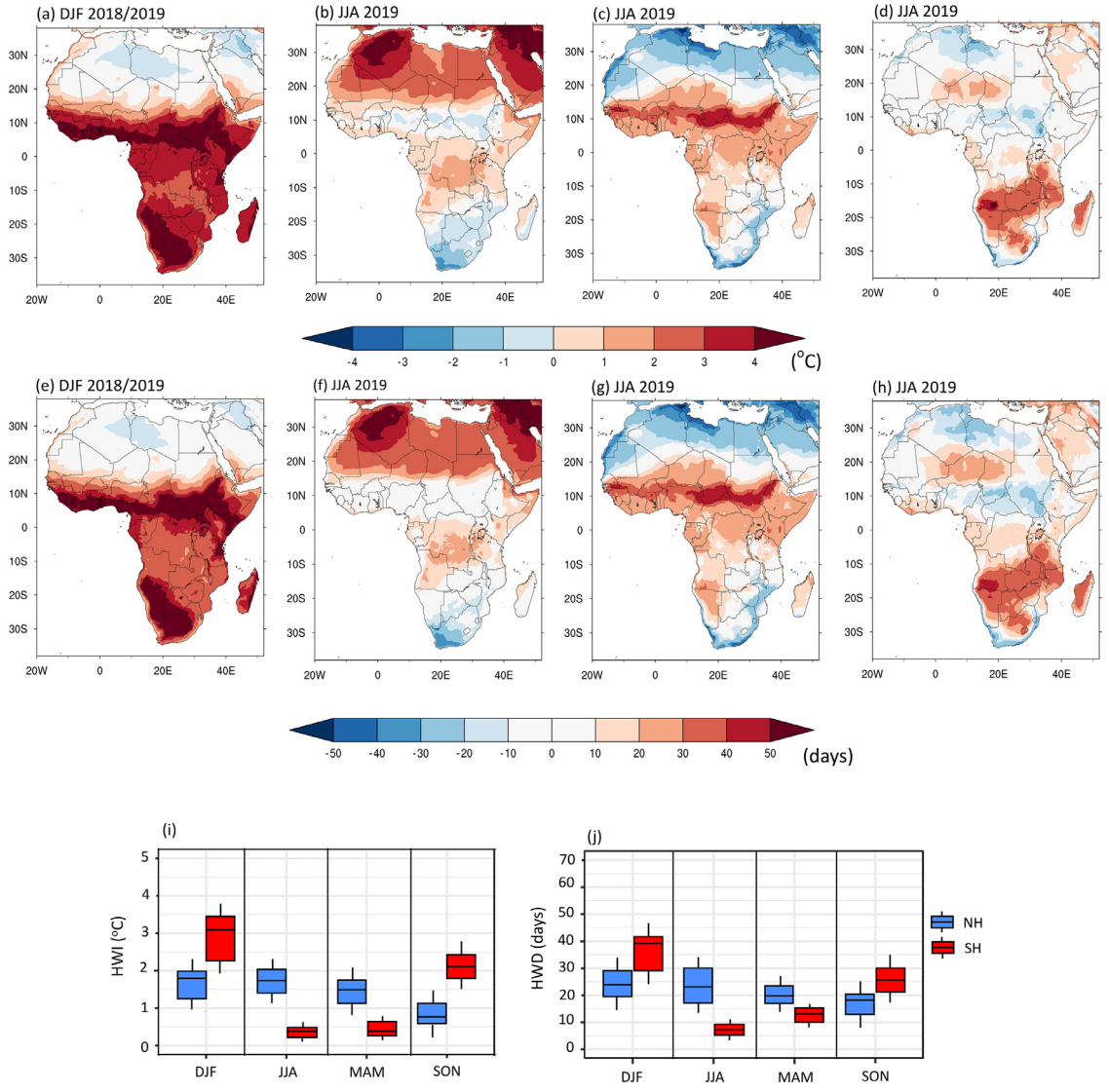

Fig. 2. Seasonal characteristics of 2019 heatwave events in the NH and SH: (a–d) 2019 anomalous HWI (units: °C) relative to the 1981–2010 baseline period for DJF, JJA, MAM and SON, respectively; (e–h) 2019 anomalous HWD (days) relative to the 1981–2010 baseline for DJF, JJA, MAM, and SON, respectively. Box-and-whisker plots indicate the 10th, 25th, 50th, 75th, and 90th quantiles of 2019 (i) seasonal HWI and (j) seasonal HWD.

3.2. Heatwave hotspots and urban area exposure in 2019

There was a major shift in the spatial distribution of heatwave hotspot areas in 2019 compared to the baseline period (Fig. 3(a, b)). Hotspots of heatwave events were located around the equatorial region in the baseline period, while in 2019 they extended to large areas in the NH and SH up to the temperate climate zones (above 30°N and 30°S). The observed heatwave hotspot areas in 2019 demonstrated by ERA5 and MODIS LST were somewhat consistent in western-coastal, southern, northwestern, and equatorial parts of Africa (Fig. S3(a, b)). However, they were inconsistent over the equator and some parts of the NH. In relation to the baseline period, the SH experienced more expansion (18%) of land areas of extreme heatwaves (99th percentile) than the NH (5%) in 2019 (Fig. 3(c)).

Across Africa in 2019, most heatwave hotspot areas were linked to the location of urban areas (Fig. 3(a, b)). The proportion of urban agglomerations (population) exposed to extreme (99th percentile) heatwaves in the NH rose from 4% (5 million people) in the baseline period to 36% (43 million people) in 2019 (Fig. 3(d)). In the SH, the exposure of urban agglomerations (population) to extreme heatwave events grew from 15% (17 million people) in the baseline period to 57% (53 million people) in 2019 (Fig. 3(e)). None of the urban agglomerations in the temperate climate zone was in an extreme heatwave area in the baseline period; however, in 2019, most of them were (up to 70%). In addition, the proportion of urban agglomerations in non-heatwave areas in the NH (SH) decreased significantly from 63% (61%) in the baseline period to 8% (3%) in 2019 (Fig. 3(d, e)). This shows that a large number of urban agglomerations were found in heatwave hotspot areas in 2019.

3.3. Mechanisms related to heatwave events in 2019

Seasonal changes in patterns of heatwave events in 2019 were related to atmospheric circulation (850-hPa HGT) and SST (Fig. 4(a–h)). In austral summer (DJF), positive HGT anomalies were observed in the south of the NH, extending also to large parts of the SH; whereas, in contrast, negative anomalies were found northward in the NH (Fig. 4(a)). In boreal summer, positive HGT anomalies were found in the north of the NH, while negative anomalies extended through most parts of the SH (Fig. 4(b)). In austral fall and austral spring, positive HGT anomalies were found southward in the SH and NH, respectively (Fig. 4(c, d)). Generally, most regions of positive/negative patterns of seasonal heat-

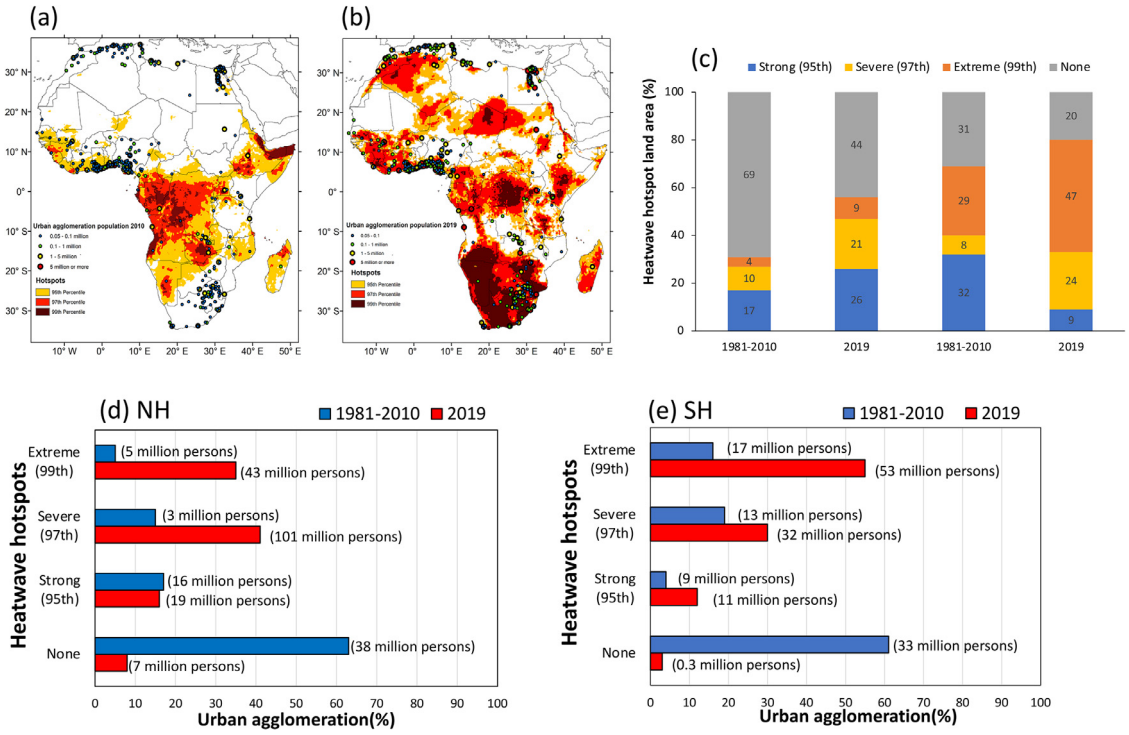

Fig. 3. Hotspots of heatwave events and urban agglomerations: (a) baseline period (1981–2010); (b) 2019; (c) land areas of heatwave hotspots; (d, e) percentage of urban agglomerations and total population in heatwave hotspot areas in the (d) NH and (e) SH.

waves and HGT agreed, with pattern correlation coefficients of 0.92, 0.81, 0.91, and 0.84 in the NH and 0.97, 0.89, 0.96, and 0.87 in the SH for DJF, MAM, JJA, and SON, respectively. Also, seasonal changes in Africa's regional SST were highly above-normal in 2019 (Fig. 4(e–h)), with peak values (up to 3°C) in boreal summer. Across all seasons, the circulation patterns (850-hPa wind) showed warm advection from positive SST regions (Fig. 4(e–h)) to land areas where heatwave events were recorded (Fig. 2(a–h)). The boreal summer was notable because easterly and westerly winds blew in from the equatorial Indian and Atlantic oceans, bringing warm air to the central and southern regions (Fig. 4(e)). Most regions of positive/negative HGT anomalies corresponded to regions of negative/positive soil moisture and precipitation anomalies across all seasons (Fig. S4(a–h)), implying that seasonal circulation patterns likely influenced dry conditions over land.

4. Discussion

The year 2019 was reported as a remarkably hot year in various regions (Xu et al., 2020; Vautard et al., 2020), and our study provides compelling evidence that Africa was no exception given the widespread heatwave events that occurred there across all seasons. Compared to the baseline period, the magnitude of heatwave events was stronger in 2019. Also, there was a major shift in the spatial distribution of heatwave hotspots from the equatorial region in the baseline period (1981–2010) to large areas up to the temperate climate zones (above 30°N and 30°S) in 2019, affecting more urban agglomerations.

We found stronger heatwave events in austral summer, and with large spatial extent (up to 60% of the total land area), compared to other seasons. This is in agreement with a previous study in which major heatwave events were observed in austral summer 2004/05 (33% of the total land area) and 2009/10 (55% of the total land area) over Africa (Russo et al., 2016). This is likely a signal of emerging stronger heatwave events across more land areas in austral summer than the widely studied boreal summer months over Africa.

We also observed above-normal atmospheric circulation across all seasons, which indicated intense warming at the surface in 2019 in relation to the baseline period. Also, the global ocean heat content attained a new record-high (Cheng et al., 2020). Specifically, heat content increased in the Pacific, Atlantic, and Indian oceans, linked to extreme climate events across the globe in 2019 (Meyssignac et al., 2019). This agrees with our study, which found above-normal regional SST and advection of warm air over land areas where major heatwaves were recorded in 2019. It is reasonable to argue that warmer SST was likely an integral part of the 2019 heatwaves in Africa. Also, the observed seasonal change in atmospheric circulation likely induced dry conditions (reduced precipitation and a soil moisture deficit) over land. This pattern is similar to a recent study (Sousa et al., 2020) that demonstrated atmospheric circulation reduces soil moisture over land during heatwaves.

We found more urban agglomerations exposed to extreme heatwaves (99th percentile) in 2019 compared to the baseline period. This highlights the increasing risks posed by heat events in highly populated urban areas, which may become inhabitable by the end of the century (Hansen and Sato, 2016). The increase in heat during heatwaves in urban areas can increase the level of heat stress as well as water and energy demands (Zhao et al., 2018). Considering the rapid population growth and urbanization in Africa, heatwave events may place further pressure on existing water and energy shortages (Wamsler et al., 2013). By identifying hotspots, this study shows regions where climate adaptation strategies are currently needed. It is also relevant to the recent focus on multi-hazard impact-based forecasting by the WMO, which attempts to identify possible impacts of recent extreme events on humans and ecosystems.

It is important to acknowledge that there are limitations to the ERA5 reanalysis dataset, such as inappropriate separation of ocean temperature from land temperature in coastal regions (Bengtsson et al., 2004). Also, limited ground observation stations in reanalysis datasets and differences in spatial resolution may have led to slight inconsistencies in the representation of heatwave hotspots (particularly over the equator

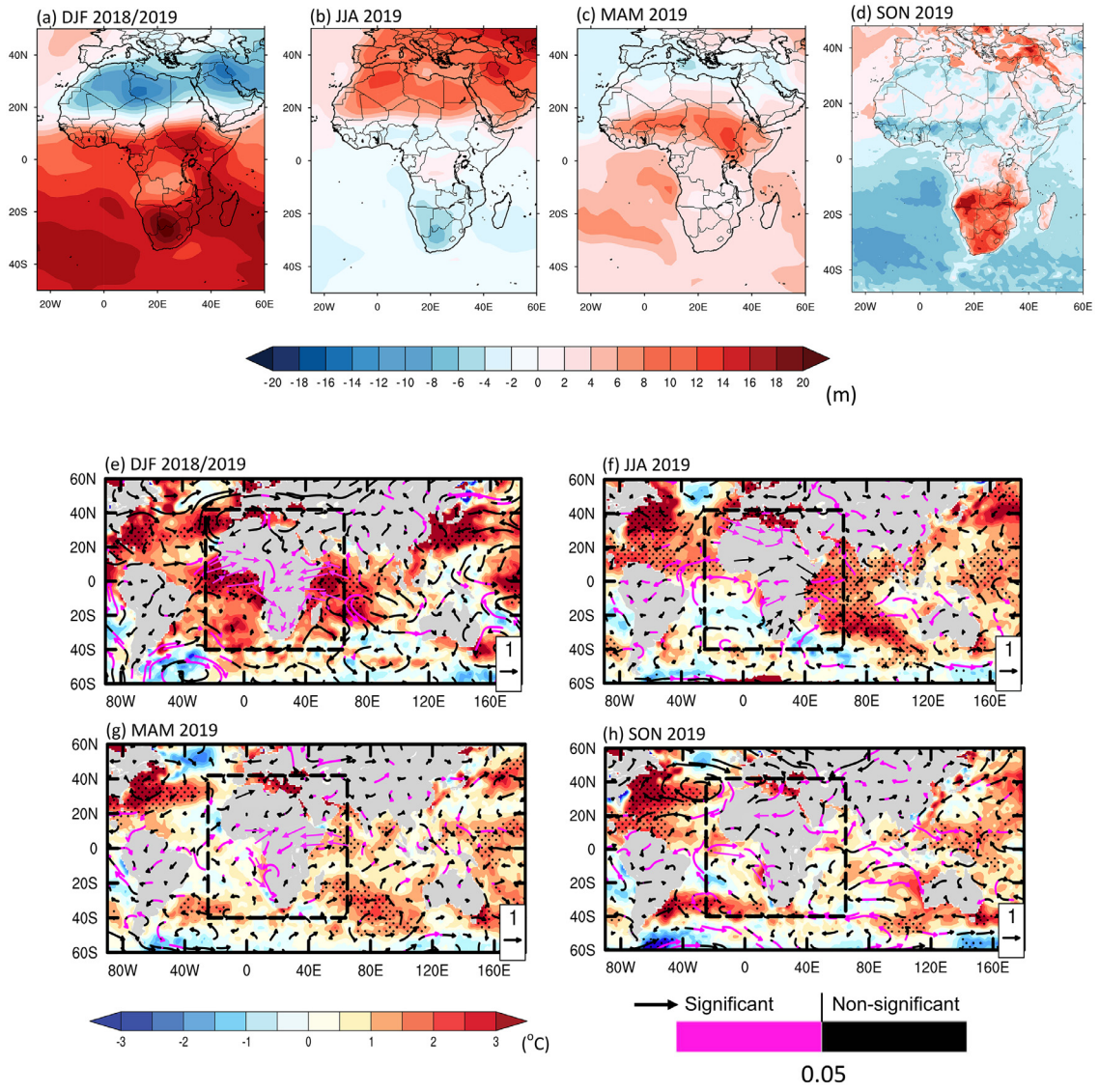

Fig. 4. The 2019 seasonal (DJF, JJA, MAM, and SON) anomalies relative to the 1981–2010 baseline period: (a–d) 850-hPa HGT; (e–h) SST (shaded) and 850-hPa wind (vectors). Stippling and magenta vectors indicate significance at the 0.05 level. Africa's regional SST is defined by the black dashed box.

and in some parts of the NH) for ERA5 and MODIS LST. Nonetheless, since reanalysis data provide comprehensive energy budget feedbacks that regulate temperature anomalies, they remain useful for analyzing climate extremes and also to reproduce patterns and trends of heatwave events over Africa (Oueslati et al., 2017).

5. Conclusion

By integrating multiple datasets to quantify recent heatwave events over Africa, we found that stronger heatwave events occurred in 2019 compared to the baseline period (1981–2010). There was a major shift in the spatial distribution of heatwave hotspots from equatorial Africa in the baseline period (1981–2010) up to temperate climate zones (above 30°N and 30°S) in 2019. Heatwave hotspot areas were clearly linked to urban agglomerations, particularly in western-coastal, northeastern, southern, and equatorial Africa, where the vast majority of the human population is located. The proportion of urban agglomerations (population) exposed to extreme (99th percentile) heatwaves in the NH and SH rose from 4% (5 million people) and 15% (17million people), respectively, in the baseline period to 36% (43 million people) and 57% (53 million people), respectively, in 2019. Heatwave events in 2019 were associated with seasonal change in anomalous SST and atmospheric circulation, likely as a result of large-scale forcing due to climate change. Considering the continuous trend of climate change and urbanization in Africa, risks posed by heatwave events will likely increase in the coming years, especially in populated areas where adaptation efforts are needed. We therefore advocate the need for urban planning with innovative solutions to help minimize heatwave exposure in Africa.

Declaration of competing interest

The authors declare no conflicts of interest.

Funding

This research was funded by the National Natural Science Foundation of China [grant numbers 41861124005 and 41675079], and the first author was a recipient of a research studentship provided by the CAS-TWAS President fellowship.

Supplementary materials

Supplementary material associated with this article can be found, in the online version, at doi:10.1016/j.aosl.2022.100195.

References

Arguez, A., Vose, R.S., 2011. The definition of the standard WMO climate normal: The key to deriving alternative climate normals. Bull. Am. Meteorol. Soc. 92, 699–704. doi:10.1175/2010BAMS2955.1.

Bengtsson, L., Hagemann, S., Hodges, K.I., 2004. Can climate trends be calculated from reanalysis data? J. Geophys. Res.: Atmos. 109, 1–7. doi:10.1029/2004JD004536.

Brooke, A.G., Bell, M.L., 2011. Heatwaves in the United States: Mortality risk during heatwaves and effect modification by heatwave characteristics in 43 U.S. communities. Environ. Health Perspect 119, 210–218. doi:10.1289/ehp.1002313.

Cheng, L., Abraham, J., Zhu, J., Trenberth, K.E., Fasullo, J., Boyer, T., Locarnini, R., et al., 2020. Record-setting ocean warmth continued in 2019. Adv. Atmos. Sci. 37, 137–142. doi:10.1007/s00376-020-9283-7.

Driouech, F., ElRhaz, K., Moufouma-Okia, W., Arjdal, K., Balhane, S., 2020. Assessing future changes of climate extreme events in the CORDEX-MENA region using regional climate model ALADIN-Climate. Earth Syst. Environ. 4, 477–492. doi:10.1007/s41748-020-00169-3.

Engelbrecht, F., Adegoke, J., Bopape, M.J., Naidoo, M., Garland, R., Thatcher, M., McGregor, J., et al., 2015. Projections of rapidly rising surface temperatures over Africa under low mitigation. Environ. Res. Lett. 10, 1–4. doi:10.1088/1748-9326/10/8/085004.

Hansen, J., Sato, M., 2016. Regional climate change and national responsibilities. Environ. Res. Lett. 11, 2–8. doi:10.1088/1748-9326/11/3/034009.

Hobday, A.J., Oliver, E.C.J., Gupta, A.Sen, Benthuysen, J.A., Burrows, M.T., Donat, M.G., Neil, J., et al., 2018. Categorizing and naming marine heatwaves. Oceanography 31, 162–173. doi:10.5670/oceanog.2018.205.

Huang, B., Banzon, V.F., Freeman, E., Lawrimore, J., Liu, W., Peterson, T.C., Smith, T.M., et al., 2015. Extended reconstructed sea surface temperature version 4 (ERSST.v4). Part I: Upgrades and intercomparisons. J. Clim. 28, 911–930. doi:10.1175/JCLI-D-14-00006.1.

Jézéquel, A., Yiou, P., Radanovics, S., 2018. Role of circulation in European heatwaves using flow analogues. Clim. Dyn. 50, 1145–1159. doi:10.1007/s00382-017-3667-0.

Lewis, S.C., King, A.D., Perkins-Kirkpatrick, S.E., Mitchell, D.M., 2019. Regional hotspots of temperature extremes under 1.5 ˚C and 2 ˚C of global mean warming. Weather Clim. Extrem. 26, 2–8. doi:10.1016/j.wace.2019.100233.

Meyssignac, B., Boyer, T., Zhao, Z., Hakuba, M.Z., Landerer, F.W., Stammer, D., Köhl, A., et al., 2019. Measuring global ocean heat content to estimate the earth energy imbalance. Front. Mar. Sci. 10, 1–9. doi:10.3389/fmars.2019.00432.

Moron, V., Oueslati, B., Pohl, B., Rome, S., Janicot, S., 2016. Trends of mean temperatures and warm extremes in northern tropical Africa (1961-2014) from observed and PPCA-reconstructed time series. J. Geophys. Res. 121, 5298–5319. doi:10.1002/2015JD024303.

Nangombe, S.S., Zhou, T., Zhang, W., Zou, L., Li, D., 2019. High-Temperature Extreme Events Over Africa Under 1.5 and 2 ˚C of Global Warming. J. Geophys. Res.: Atmos. 124, 4413–4428. doi:10.1029/2018JD029747.

Oueslati, B., Pohl, B., Moron, V., Rome, S., Janicot, S., 2017. Characterization of heatwaves in the Sahel and associated physical mechanisms. J. Clim. 30, 3095–3115. doi:10.1175/JCLI-D-16-0432.1.

Perkins, S.E., Alexander, L.V., 2013. On the measurement of heatwaves. J. Clim. 26, 4500–4517. doi:10.1175/JCLI-D-12-00383.1.

Rohat, G., Johannes, F., Alessandro, D., Hy, D., van-Maarseveen, M., 2019. Projections of Human Exposure to Dangerous Heat in African Cities Under Multiple Socioeconomic and Climate Scenarios. Earth's Fut 7, 528–546. doi:10.1029/2018EF001020.

Russo, S., Dosio, A., Graversen, R.G., Sillmann, J., Carrao, H., Dunbar, M.B., Singleton, A., Montagna, P., Barbola, P., Vogt, J.V., 2014. Magnitude of extreme heatwaves in present climate and their projection in a warming world. J. Geophys. Res.: Atmos. 119, 500–512. doi:10.1002/2014JD022098.

Russo, S., Marchese, A.F., Sillmann, J., Immé, G., 2016. When will unusual heatwaves become normal in a warming Africa? Environ. Res. Lett. 20, 12–15. doi:10.1088/1748-9326/11/5/054016.

Sousa, P.M., Barriopedro, D., García-Herrera, R., Ordonez, C., Soares, P.M.M., Trigo, R.M., 2020. Distinct influences of large-scale circulation and regional feedbacks in two exceptional 2019 European heatwaves. Commun. Earth Environ. 1, 46–48. doi:10.1038/s43247-020-00048-9.

Vautard, R., Van Aalst, M., Boucher, O., Drouin, A., Haustein, K., Kreienkamp, F., Van Oldenborgh, G.J., et al., 2020. Human contribution to the record-breaking June and July 2019 heatwaves in Western Europe. Environ. Res. Lett. 15, 1–31. doi:10.1088/1748-9326/aba3d4.

Wamsler, C., Brink, E., Rivera, C., 2013. Planning for climate change in urban areas: From theory to practice. J. Clean. Prod. 50, 68–81. doi:10.1016/j.jclepro.2012.12.008.

Wan, Z., 2008. New refinements and validation of the MODIS Land-Surface Temperature/Emissivity products. Remote Sens. Environ. 112, 59–74. doi:10.1016/j.rse.2006.06.026.

Weedon, G.P., Balsamo, G., Bellouin, N., Gomes, S., Best, M.J., Viterbo, P., 2014. The WFDEI meteorological forcing data set: Watch Forcing Data methodology applied to ERA-Interim reanalysis data. Water Resour. Res. 50, 7505–7514. doi:10.1002/2014WR015638.

Wilhelmi, O.V., Hayden, M.H., 2010. Connecting people and place: A new framework for reducing urban vulnerability to extreme heat. Environ. Res. Lett. 5, 10–13. doi:10.1088/1748-9326/5/1/014021.

Zhao, L., Oppenheimer, M., Zhu, Q., Baldwin, J.W., Ebi, K.L., Bou-Zeid, E., Guan, K., Liu, X., 2018. Interactions between urban heat islands and heatwaves. Environ. Res. Lett. 13, 1–9. doi:10.1088/1748-9326/aa9f73.

Xu, P., Wang, L., Liu, Y., Chen, W., Huang, P., 2020. The Record-Breaking Heat Wave of June 2019 in Central Europe. Atmos. Sci. Lett. 21, 1–5. doi:10.1002/asl.964.